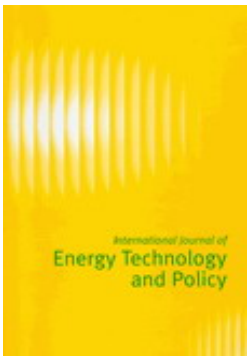

International Journal of Energy Technology and Policy

ISSN online: 1741-508X - ISSN print: 1472-8923
https://www.inderscience.com/ijetp

The dynamic impact of regional construction industry economy, energy and carbon emissions based on HMM

Guangquan Zhou, Zhiyu Fu, Yong Liu, Zhengya He, Mengya Cai, Liang Luo

DOI: 10.1504/IJETP.2024.10062210

Article History:

Received:	23 May 2023
Last revised:	19 June 2023
Accepted:	19 October 2023
Published online:	10 May 2024

The dynamic impact of regional construction industry economy, energy and carbon emissions based on HMM

Guangquan Zhou*

Anhui Province Key Laboratory of Green Building and Assembly Construction, Anhui Institute of Building Research and Design, Heifei, Anhui, 230031, China
and
School of Civil Engineering, Nanchang Hangkong University, Nanchang, 330063, China
Email: guangqu66@mls.sinanet.com
*Corresponding author

Zhiyu Fu

School of Civil Engineering, Nanchang Hangkong University, Nanchang, 330063, China
Email: Zhiyu@mls.sinanet.com

Yong Liu

Beijing Public Highway Link Co., Ltd., Beinjing, 100161, China
Email: YongLiu@mls.sinanet.com

Zhengya He and Mengya Cai

Anhui Province Key Laboratory of Green Building and Assembly Construction, Anhui Institute of Building Research and Design, Heifei, Anhui, 230031, China
Email: Zhengya@mls.sinanet.com
Email: Mengya@36haojie.com

Liang Luo

School of Civil Engineering, Nanchang Hangkong University, Nanchang, 330063, China
Email: LiangLuo@36haojie.com

Abstract: Aiming at the uncertainty of the internal correlation between economic growth, energy consumption and carbon emissions in regional construction industry, a dynamic impact research method based on hidden Markov model (HMM) was proposed. Firstly, the dynamic correlation of three variables in the region was established based on HMM, the optimisation parameter estimation of time window was set, and the optimal prediction of carbon emission state was achieved with Viterbi algorithm. Then, the dynamic parameters of the model with the best prediction effect were obtained, and further describes the evolution of the interaction of the three variables in the region. Finally, the empirical analysis of the East China region shows that the average prediction accuracy of HMM under the optimal time window is more than 93%, and its dynamic parameters intuitively describe the change in regional carbon emission development state and the dynamic relationship between carbon emissions, economic growth, and energy consumption.

Keywords: building carbon emissions; improved HMM; state prediction; dynamic impact.

Reference to this paper should be made as follows: Zhou, G., Fu, Z., Liu, Y., He, Z., Cai, M. and Luo, L. (2024) 'The dynamic impact of regional construction industry economy, energy and carbon emissions based on HMM', *Int. J. Energy Technology and Policy*, Vol. 19, Nos. 1/2, pp.17–34.

Biographical notes: Guangquan Zhou received his Master's in Civil Engineering Planning and Management from the School of Civil Engineering and Architecture of Central South University, and PhD in Road and Railway Engineering from the same school in 2018. He is currently an Associate Professor in the School of Civil Engineering and Architecture of Nanchang Hangkong University. His research interests include project management, intelligent buildings, etc.

Zhiyu Fu received her Bachelor's in Engineering Management from the School of Civil Engineering and Architecture of Nanchang Hangkong University. At present, she is a Master's student at Nanchang Hangkong University. Her research interests include low-carbon building and intelligent construction.

Yong Liu graduated from the School of Civil Engineering and Architecture of Central South University with a Bachelor's in Engineering Management. At present, he is a Comprehensive Management Engineer in the planning and contract department of Beijing Gonglian Highway Link Co., Ltd., mainly engaged in building economic analysis, project contract management and so on.

Zhengya He received his Bachelor's in Electronic Information Engineering from School of Anhui Jianzhu University, and Master's in Municipal Engineering from the same school in 2011. He is currently a Senior Engineer in the Anhui Institute of Building Research and Design. His research interests include green building low-carbon and reduced carbon technology, energy efficiency improvement of existing building, and energy audit.

Mengya Cai received her Master's in Geological Engineering from Anhui University of Science and Technology in 2018. She is currently an Engineer in Anhui Institute of Building Research and Design. Her research interests include construction engineering and municipal engineering.

Liang Luo received his Master's in Civil Engineering from School of Urban construction of Yunnan University, and PhD in Civil Engineering from School Civil Engineering of Central South University in 2019. He is currently a Lecturer in the School of Civil Engineering and Architecture of Nanchang Hangkong University. His research interests include mechanics, structural engineering and construction technology.

1 Introduction

Sustainable development is the responsibility and unwavering pursuit of all nations in the world since high-quality economic growth, energy efficiency, and a healthy ecological environment are interdependent (Liu et al., 2019; Ye et al., 2023). One of the implications of China's pursuit of high-quality development is ensuring stable economic growth while meeting the objectives of energy control and carbon emission reduction (Dong and Chang, 2023). China has consistently shown that it is willing to actively combat climate change and move in the direction of a low-carbon future. The Chinese Government vowed solemnly in 2015 to cut its carbon emission intensity by 60% to 65% by 2030 in comparison to 2005 (Xie, 2021). In 2020, China's carbon peaking and carbon neutrality goals are officially proposed (Li and Li, 2020). At the moment, carbon emission has become a significant determinant of energy policies, and it is also necessary to promote the synchronous development of economic growth and carbon dioxide decoupling. The focus of relevant policy planning in various countries is on how to achieve the coordinated development of the combined system of economic growth, energy consumption, and carbon emission (Huang et al., 2021).

Carbon emissions must be under control in energy-intensive industries in order to maintain sustainable development (Du et al., 2019). Due to its enormous growing development approach, the construction industry has over the past few years grown to be one of the three largest consumers of energy in China. The added value of the construction industry contributed more than 6.6% of the GDP during the 13th Five-Year Plan period, and in 2021, it has contributed to 7% (Statistics Bureau of the People's Republic of China, 2021). The building industry's energy use and carbon emissions are increasing along with the economy's growth. In 2015, Chinese buildings consumed 857 million tons of standard coal, which accounted for 25% of the nation's total energy consumption (Li et al., 2017). By 2019, the whole construction process had consumed 2.233 billion tons of standard coal, comprising 45.8% of China's total energy consumption. Additionally, the process contributed 4.997 billion tons of carbon dioxide, representing 49.97% of the national carbon emission (CABBE, 2021). It is estimated that carbon emissions from construction processes will increase by 2.7% to reach 5.22 billion tons of carbon dioxide by 2021 (CABBE, 2021). Controlling energy consumption, reducing carbon emissions, and supporting sustainable economic progress pose significant challenges for the construction industry. China's varying resources, economic development, and technical expertise necessitate coordinated regional development as a central national strategy (Sun and Zhang, 2021), with the construction industry's overall efforts being vital to achieve this goal (Yan and Chen, 2022).

Energy is the foundation of economic development and the primary source of carbon emissions. Numerous theoretical and empirical studies have examined the relationship

and causality between economic growth, energy consumption, and environmental levels, usually expressed by variables such as GDP, per capita GDP, total industrial output value, energy consumption, energy efficiency, carbon emissions, and sulphur dioxide emissions (Ye et al., 2023). Granger causality models, vector autoregressive (VAR), and vector error correction model (VECM) are commonly utilised to analyse the simultaneous effects of the three (Adedoyin and Bekun, 2020; Jebli and Youssef, 2017), while carbon emission intensity and carbon emission efficiency are evaluation indicators widely used to reflect the relationship between the three. Due to different research fields and geographical regions selected, there are certain differences in causality, influence degree and influence time (Ye et al., 2023; Li et al., 2019).

For predicting changes among the three, the environmental Kuznets curve (EKC) was proposed as an idealised representation of the relationship between economic development and environmental quality, with an inverted U-shaped curve (Grossman and Krueger, 1995). However, the decoupling analysis is more practical and easy to calculate compared to the EKC and can identify the changes of variables over time (Yan and Chen, 2022; Dong et al., 2020). Besides machine learning methods such as artificial neural networks, support vector machines, and recurrent neural networks show great potential (Wen and Yuan, 2020; Ağbulut, 2022). However, the improvement of prediction accuracy largely depends on a large number of historical data. Considering that the time series prediction requires a large amount of data and stable distribution, Ye et al. (2023) adopted the grey system model to model and forecast the interaction between the three, and introduced a dynamic compensation mechanism to adapt to the interactive system of economy, energy and environment. The grey system model has good adaptability to the prediction of unknown systems.

With the development of spatial econometrics and related software, the analytical perspective gradually extends to spatial dimensions, and variables such as Moran index, Thiel index, threshold coefficient, coefficient of variation, and nuclear density are utilised to examine the spatial characteristics of the three indexes (Wang et al., 2021). Panel vector autoregressive (PVAR) and global vector autoregressive (GVAR) models can assess the spatial and temporal dynamics of the three substantially (Serdar et al., 2023; Assis et al., 2023), while the spatial Markov model adds a spatial lag term to the traditional Markov model, enabling a quantifiable analysis of the long-term spatial spillover effect between regions (Rey, 2001). Wang et al. (2019) used the spatial Markov transition probability matrix to predict the changing trend of carbon emission intensity. Du et al. (2022) applied it to explore the regional distribution pattern of carbon emission efficiency, and revealed the dynamic interaction among provinces through the transfer probability analysis of carbon emission efficiency. For the prediction of spatial evolution, Lin and Yu (2016) adopt the hidden Markov model (HMM) to model the traffic distribution on the network topological space, and by predicting the link load, make the link that is most likely to be idle enter the sleep mode to save energy. The prediction advantage of this method is that it does not need to obtain a large amount of data and can easily adapt to real-time scenarios (Manouchehri and Bouguila, 2023). It is widely used in speech recognition, image processing, information, machinery, transportation, biology and other fields (Elmezain et al., 2023; Ulmeanu et al., 2017). Since the state transition matrix estimation of HMM is calculated from the accumulated historical data, it cannot show the real-time state changes of the observing process and the hidden process. Some scholars have effectively solved this problem by setting a sliding time window (Wang et al., 2018).

In conclusion, there exists a clear and intricate interdependence among economic development, energy consumption, and carbon emissions, which is perpetually evolving. The interaction among these three constructs, along with the corresponding evaluation metrics, displays distinct spatial characteristics impacting the degree of interaction. Several challenges remain, however, such as the limited attention paid to forecasts derived from the interaction relationship despite extensive research (Ye et al., 2023). Moreover, the calculation of total carbon emissions from energy consumption varies among industries due to disparate carbon dioxide conversion coefficients for different energy sources. Publication of authoritative data slightly lags behind data on energy consumption and economic growth, contributing to greater uncertainty in establishing dynamic change models for interaction among the three factors. Existing studies in the field of architecture have mainly utilised the spatial Markov model, which analyses spillover effects on a single indicator, but is limited in providing real-time information feedback to quickly capture the impact of changes in external environments and policy incentives (Manouchehri and Bouguila, 2023).

HMM contains an observable random process and a hidden random process. The establishment of HMM from a spatial perspective can comprehensively consider the correlation between time, space and factors, and provide a good framework for analysing the correlation changes of economic growth, energy consumption and carbon emissions in the construction industry region. Therefore, a dynamic correlation change research method based on HMM is proposed. Based on the lag of carbon emission data, the state change of carbon emission data is regarded as a hidden process, and the state change of economic growth and energy consumption is regarded as an observed process. Using the change of the number of regions with a certain state of the three, the changes of the whole three regions and their interaction effects are represented, and the three-variable dynamic correlation HMM from the spatial perspective is constructed. Taking the prediction accuracy of hidden variables as the index, the time window is set to optimise the HMM parameter training and prediction, and the Viterbi algorithm is used to explore the best fitting of the dynamic change of regional three variables. At this time, HMM dynamic parameters can better characterise the dynamic correlation evolution process among the three.

The following structure of this paper is divided into three parts. In Section 2, the basic concept of HMM and the research method of spatial HMM based on time window are introduced. In Section 3, the validity of the proposed method is verified by an empirical analysis of the actual time series data in East China region. Finally, a conclusion was made.

2 Construction of regional HMM

2.1 Introduction to HMM

For reference to Sosiawan et al. (2021), the HMM mainly consists of an hidden state sequence $S = \{s_1, s_2,\ldots, s_T\}$ and an observation state sequence $O = \{o_1, o_2,\ldots, o_T\}$, and T is the total length of the time sequence. The hidden state sequence contains a total of N classes of hidden states, denoted as the set $Q = \{q_1, q_2,\ldots, q_N\}$ and the observation state sequence contains M classes of observation states, denoted as the set $V = \{v_1, v_2,\ldots, v_M\}$. The HMM parameters can be represented by $\lambda = \{A, B, \Pi\}$, where:

1 $A = [\alpha_{ij}]_{N\times N}$ is the hidden state transfer probability matrix, where $\alpha_{ij} = P(s_{t+1} = q_j \mid s_t = q_i)$ $(i, j \in (1, 2, \ldots, N))$ and $\sum_{j=1}^{N} \alpha_{ij} = 1$, denotes the probability of transitioning the hidden state q_i at moment t to the hidden state q_j at moment $t + 1$.

2 $B = [b_j(k)]_{N\times M}$ is the observation state transfer probability matrix, where $b_j(k) = P(o_t = v_k \mid s_t = q_j)$ $(j \in (1, 2, \ldots, N), k \in (1, 2, \ldots, M))$ and $\sum_{k=1}^{M} b_j(k) = 1$, denotes the probability that the hidden state q_j corresponds to the observation state transfer probability matrix state v_k at moment t.

3 $\Pi = (\pi_1, \pi_2, \ldots, \pi_N)$ is the initial state probability distribution, which indicates the probability of occurrence of the hidden state q_i at the beginning of the HMM, i.e., $t = 1$, and $\sum_{i=1}^{N} \pi_i = 1$.

Figure 1 HMM process (see online version for colours)

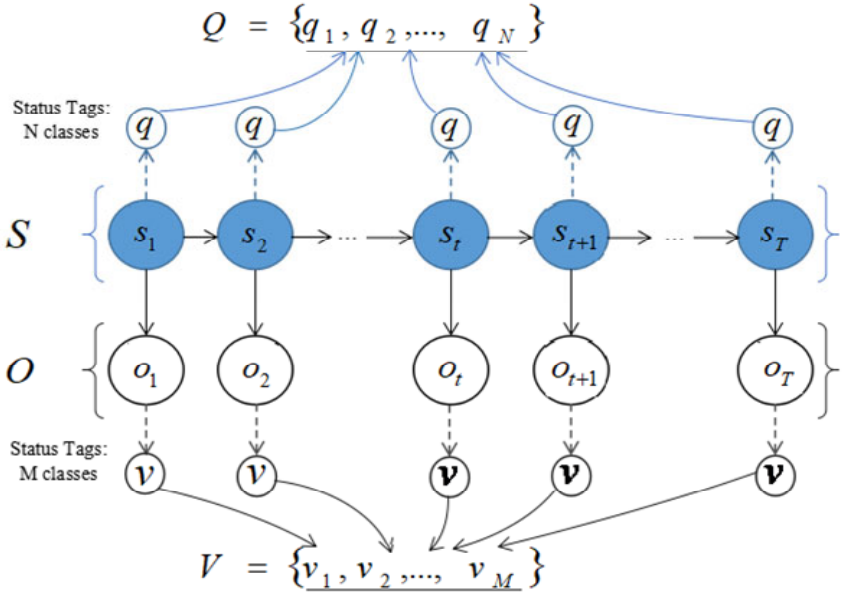

2.2 Spatial HMM

Build the HMM from the spatial dimension. Suppose there are a provinces in the region, including a HMMs. calculate the parameters with the relative frequency of the occurrence and change of hidden state and observed state from moment t to moment $t = 1$. The number of regions where hidden state q_i appears at moment t is $(0 \le a_{q_i(t)} \le a)$, where hidden state q_j appears at moment $t + 1$ is $(0 \le a_{q_j(t+1)} \le a)$. Therefore, the initial state probability $\overline{\pi}_i = a_{q_i(t)} / a$, the state transition probability $\overline{\alpha}_{ij} = a_{q_i(t)} / a_{q_j(t+1)}$.

Similarly, suppose the number of observation states v_k at moment t is $(0 \le a_{v_k(t)} \le a)$, the observation state transfer probability $\overline{b}_{ij} = a_{v_k(t)} / a_{q_j(t)}$.

Figure 2 Multi-HMM process (see online version for colours)

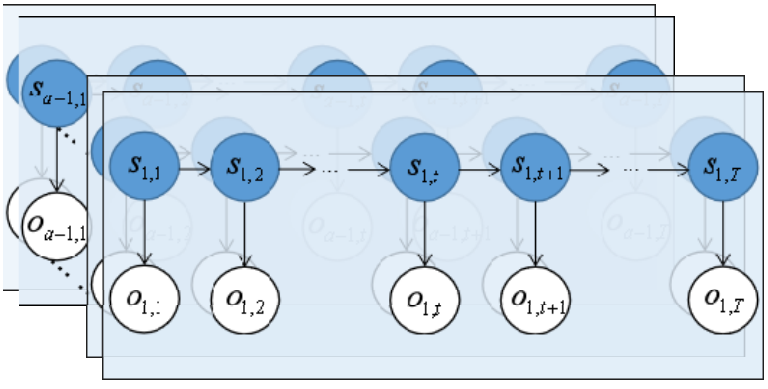

2.3 *Time windows settings*

The time window is noted as $T_{change} = (t_{pre}, t\_)$, where t_{pre} is the prediction time step and $t\_$ is the parameter training history time step. The dynamic parameters $\lambda\_ = \{A\_, B\_, \Pi\_\}$ are estimated from the observation and hidden state sequences within the window.

Figure 3 HMM process with time window (see online version for colours)

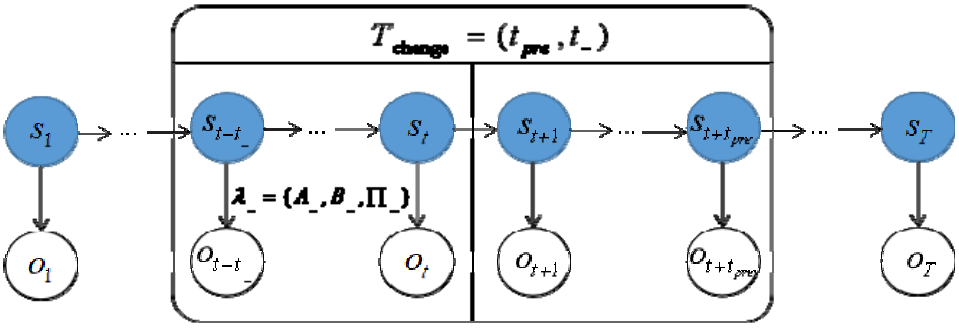

Since at least 2 consecutive years of data are required to estimate the hidden state transfer parameter A, $t_{pre} \in [1, T-2]$, $t\_ \in [2, T - t_{pre}]$. The change of time window starts with $t_{pre} = 1$, increase the prediction step size and then gradually change the parameter estimation step size $t\_$, up to $T - t_{pre}$. HMM parameters are estimated in the $t\_$ window, and Viterbi algorithm [32] is used to select the region hidden state sequence with the greatest probability in the t_{pre} window. To reflect the overall prediction effect of the region, a simple sum is used to average the prediction accuracy of each region. After finding the best prediction for the region as a whole, the dynamic parameters were used to characterise the dynamic changes among the three elements in the region.

Figure 4 Brief flowchart of the HMM method based on time window (see online version for colours)

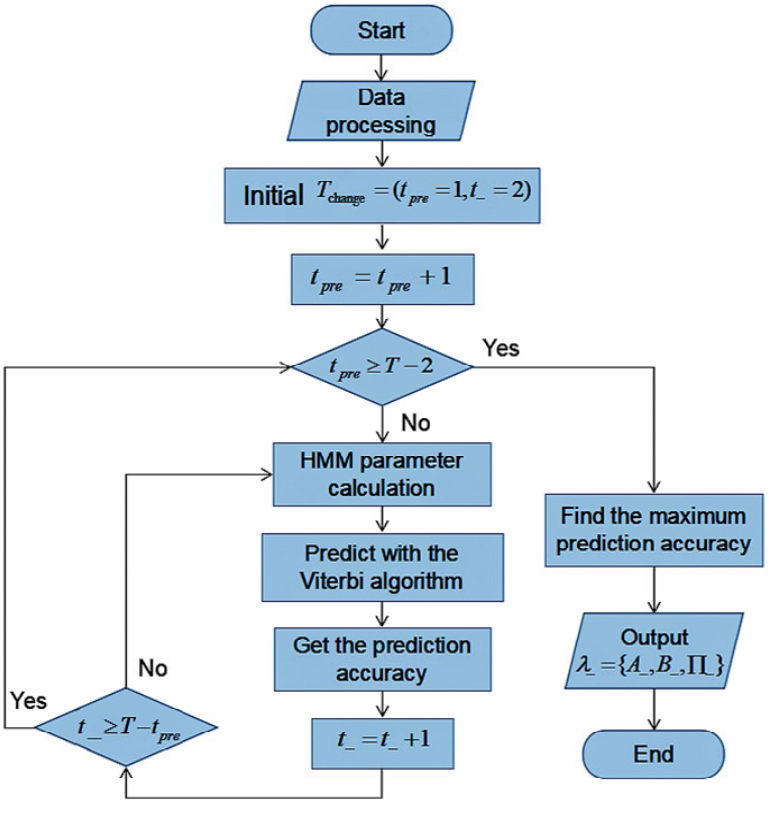

3 Empirical analysis

3.1 Data acquisition

Taking East China region as an example, time-series data were collected for seven provinces including Shanghai, Jiangsu, Zhejiang, Anhui, Fujian, Jiangxi and Shandong. The total construction output value was selected as the economic growth indicator and the regional terminal energy consumption as the energy consumption indicator, and the data on the total construction output value and energy consumption from 2005 to 2020 were collected from the China Statistical Yearbook and the China Energy Statistical Yearbook for each region. The actual regional gross output value was calculated with 2005 as the base period, the total carbon emission was accounted for by the emission factor method, and the various types of energy consumption were converted into the total amount of standard coal. Some data are shown in Table 1.

Table 1 Total construction output, total energy consumption and carbon emissions in East China, 2005–2020

Year	*Province*	*Total construction industry output (billion yuan)*	*Total energy consumption (million tons)*	*Carbon emissions (million tons)*
2005	Shanghai	1,889.25	149.87	262.97
2005	Jiangsu	4,368.95	146.78	197.62
2005	Zhejiang	4,718.74	128.19	239.64
2005	Anhui	963.54	47.25	109.58
2005	Fujian	873.98	38.97	79.15
2005	Jiangxi	566.04	11.31	29.03
2005	Shandong	2,509.10	512.32	472.02
...	...	...	...	...
2020	Shanghai	8,462.48	185.79	498.09
2020	Jiangsu	36,041.44	350.76	987.28
2020	Zhejiang	21,407.73	325.73	893.31
2020	Anhui	9,574.94	216.97	511.45
2020	Fujian	14,434.32	253.77	552.59
2020	Jiangxi	8,842.94	104.82	322.43
2020	Shandong	15,282.19	401.28	1,105.33

3.2 Model parameter estimation

The Slope value of the selected index is used to characterise its development status, and the Slope value greater than 0 is the growth status, and the status label is 1; the Slope value less than 0 is the decrease status, and the status label is –1; in practice, the occurrence of Slope = 0 can be ignored. In order to reduce the complexity of the calculation, after obtaining the Slope value of each data its logarithmic and normalisation process. The number of observation states $N = 4$ and the number of hidden states $M = 2$ of the simplified HMM, and other parameters are as follows:

$$A = \begin{bmatrix} \alpha_{11} & \alpha_{12} \\ \alpha_{21} & \alpha_{22} \end{bmatrix} \quad \text{Among them}: \begin{cases} \alpha_{11} = P(s_{t+1} = -1 \mid s_t = -1) \\ \alpha_{12} = P(s_{t+1} = -1 \mid s_t = 1) \\ \alpha_{21} = P(s_{t+1} = 1 \mid s_t = -1) \\ \alpha_{22} = P(s_{t+1} = 1 \mid s_t = 1) \end{cases} \tag{1}$$

$$B = \begin{bmatrix} b_{11} & b_{12} & b_{13} & b_{14} \\ b_{21} & b_{22} & b_{23} & b_{24} \end{bmatrix} \quad \text{Among them}: \begin{cases} b_{11} = P(o_t = [-1,-1] \mid s_t = -1) \\ b_{12} = P(o_t = [-1,1] \mid s_t = -1) \\ b_{13} = P(o_t = [1,-1] \mid s_t = -1) \\ b_{14} = P(o_t = [1,1] \mid s_t = -1) \\ b_{21} = P(o_t = [-1,-1] \mid s_t = 1) \\ b_{22} = P(o_t = [-1,1] \mid s_t = 1) \\ b_{23} = P(o_t = [1,-1] \mid s_t = 1) \\ b_{24} = P(o_t = [1,1] \mid s_t = 1) \end{cases} \tag{2}$$

$$\Pi = \begin{bmatrix} \pi_1 & \pi_2 \end{bmatrix} \quad \text{Among them}: \begin{cases} \pi_1 = P(s_t = -1) \\ \pi_2 = P(s_t = 1) \end{cases} \tag{3}$$

3.3 Analysis of experimental results

The length of the observation state data set and the hidden state data set $T = 15$, and the dynamic estimation of the parameters and the hidden state prediction of the unfolding time window are gradually changed. To increase the practical validity of the model, t_{pre} is limited to the range of [1, T / 2]; due to the small time series data in this case, $t\_$ is still taken as [2, $T - t_{pre}$].

3.3.1 Prediction results

3.3.1.1 Regional prediction correct rate

Fixed prediction step $t_{pre} = 1$, the results of HMM calculation are shown in Table 2. The average correct rate of regional carbon emission status prediction when the parameter estimation step is $t\_ = 2$ is 100%, 100%, 100%, 100%, 85.71%, 71.43%, 100%, 100%, 71.43%, 100%, 71.43%, 85.71%, 100%, 100%, and 100% in each year, respectively, with an average accuracy of 93.41%. $t\_$ when increasing gradually, the average correct rate within the same year is smaller than the effect at $t\_ = 2$. In particular, with the forecasts for 2014, 2018, and 2020, it can be seen that the model parameter estimation by taking the near time series data can better capture the effect of the observation state change with the hidden state change.

Figure 5 Comparison of the correct prediction rate of optimised HMM and traditional HMM (see online version for colours)

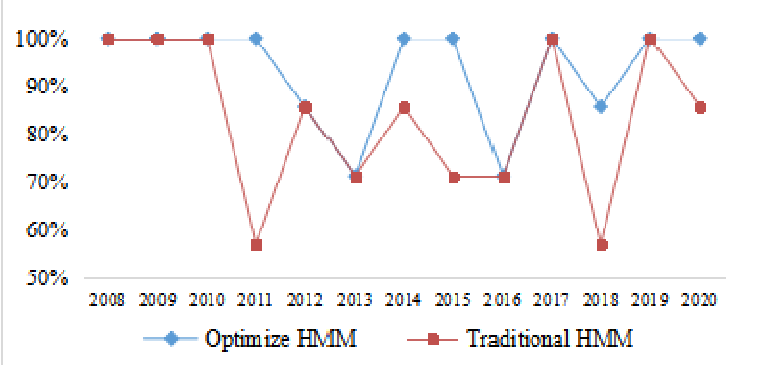

The prediction correctness of the conventional HMM is shown on the main diagonal of Table 2, and the parameter estimation interval is for all historical years data with an average correctness of 83.52%. The comparison with the correct prediction rate of HMM at $t_{pre} = 1$, $t\_ = 2$ is shown in Figure 5, and the overall prediction effect of the optimised HMM is better than that of the traditional HMM.

Table 2 Overall correct prediction rate of HMM at $t_{pre} = 1$ (unit: %)

Predict year	*t_ = 2*	*t_ = 3*	*t_ = 4*	*t_ = 5*	*t_ = 6*	*t_ = 7*	*t_ = 8*	*t_ = 9*	*t_ = 10*	*t_ = 11*	*t_ = 12*	*t_ = 13*	*t_ = 14*
2008	100												
2009	100	100											
2010	100	100	100										
2011	100	100	100	57.14									
2012	85.71	85.71	85.71	85.71	85.71								
2013	71.43	71.43	71.43	71.43	71.43	71.43							
2014	100	85.71	85.71	85.71	85.71	85.71	85.71						
2015	100	100	100	71.43	71.43	71.43	71.43	71.43					
2016	71.43	71.43	71.43	71.43	71.43	71.43	71.43	71.43	71.43				
2017	100	100	100	100	100	100	100	100	100	100			
2018	85.71	57.14	57.14	57.14	57.14	57.14	57.14	57.14	57.14	57.14	57.14		
2019	100	100	100	100	100	100	100	100	100	100	100	100	
2020	100	85.71	85.71	85.71	85.71	85.71	85.71	85.71	85.71	85.71	85.71	85.71	85.71
Average correct rate	93.41	88.09	87.01	78.57	80.95	80.36	81.63	80.95	82.86	85.71	80.95	92.86	85.71

Table 3 Overall correct prediction rate of HMM based on time window (unit: %)

t_{pre}	$t\_ = 2$	$t\_ = 3$	$t\_ = 4$	$t\_ = 5$	$t\_ = 6$	$t\_ = 7$	$t\_ = 8$	$t\_ = 9$	$t\_ = 10$	$t\_ = 11$	$t\_ = 12$	$t\_ = 13$	$t\_ = 14$
1	93.41	88.09	87.01	78.57	80.95	80.36	81.63	80.95	82.86	85.71	80.95	92.86	85.71
2	85.12	83.77	81.43	78.57	79.46	79.59	79.76	80.00	82.14	80.95	82.14	92.86	
3	80.09	78.57	79.89	77.38	78.23	77.78	78.10	78.57	77.78	78.57	76.19		
4	77.50	78.97	79.02	78.06	78.57	78.57	79.46	78.57	80.36	82.14			
5	76.83	77.14	78.78	77.62	78.29	78.57	78.10	78.57	80.00				
6	76.19	77.21	78.17	77.62	78.57	77.78	78.57	78.57					

The average correctness of the HMM with changing time windows is shown in Table 3. The overall prediction effect of the HMM gradually decreases as t_{pre} gradually increases. Some of the prediction effects improve as $t\_$ increases to equal and greater than t_{pre}. Therefore, after setting the time window in the HMM, it can be used to explore more applicable parameters in multiple ranges to improve the overall prediction effect; the time window can be selected optimally according to the needs in the face of different problems. In this example, the overall prediction effect of HMM is better with shorter parameter estimation and prediction steps, and it is more interpretable.

Table 4 Correct prediction rate of HMM regions under $T_{change} = (t_{pre} = 1, t\_ = 2)$ (unit: %)

Predict year	*Shanghai*	*Jiangsu*	*Zhejiang*	*Anhui*	*Fujian*	*Jiangxi*	*Shandong*	*Regional average accuracy*
2009	100	100	100	100	100	100	100	100
2010	100	100	100	100	100	100	100	100
2011	100	100	100	100	100	100	100	100
2012	100	100	100	100	100	100	100	100
2013	100	100	100	100	100	100	0	85.71
2014	0	100	100	100	100	100	0	71.43
2015	100	100	100	100	100	100	100	100
2016	100	100	100	100	100	100	100	100
2017	100	0	0	100	100	100	100	71.43
2018	100	100	100	100	100	100	100	100
2019	100	100	0	100	100	100	100	85.71
2020	100	100	100	100	100	100	100	100
Province average correct rate	91.67	91.67	83.33	100	100	100	83.33	

Table 5 Correct prediction rate of HMM regions under $T_{change} = (t_{pre} = 2, t\_ = 2)$ (unit: %)

Predict year	*Shanghai*	*Jiangsu*	*Zhejiang*	*Anhui*	*Fujian*	*Jiangxi*	*Shandong*	*Regional average accuracy*
2010	100	100	100	100	100	100	100	100
2011	50	50	100	100	50	100	100	78.57
2012	50	50	100	100	50	100	100	78.57
2013	50	100	100	100	100	100	0	78.57
2014	0	100	100	100	100	100	50	78.57
2015	50	50	100	100	100	100	50	78.57
2016	100	100	100	100	100	100	100	100
2017	100	50	50	100	100	100	100	85.71
2018	50	100	50	100	100	100	50	78.57
2019	50	100	0	100	100	100	50	71.43
Province average correct rate	60	80	80	100	90	100	70	

3.3.1.2 Correct prediction rate by province

The overall prediction of carbon emission status obtained by the regional HMM in the time windows $T_{change} = (t_{pre} = 1, t\_ = 2)$ and $T_{change} = (t_{pre} = 2, t\_ = 2)$ is better than 85%. The correct prediction rate of each province at this time for each region under the short time window is obtained and shown in Tables 4 and 5. The correct prediction rate of the HMM for each region under $T_{change} = (t_{pre} = 1, t\_ = 2)$ is at least 83%, and the overall performance of the HMM decreases when the prediction step size increases.

3.3.2 Analysis of regional state changes based on dynamic parameters

After step-by-step training, the time window with the best overall prediction is $T_{change} = (t_{pre} = 1, t\_ = 2)$. At this time, the regional HMM is more suitable for characterising the overall three-factor state change and transfer. The dynamic parameters obtained on the basis $\lambda\_ = \{A\_, B\_, \Pi\_\}$ for the period from 2007 to 2019 are obtained as shown in Figures 6, 7 and 8.

1 Change in carbon emission development status

The change in the hidden state shift probability from Figure 6(a) shows that the probability of carbon emission state change to lowering has increased from 2009 to 2013, and the development of carbon emission has decelerated in all parts of East China region during this time period. α_{21} denoted as the change in probability of state from growth to lowering, the trend shows that after 2009, the regions that changed from growth to lowering state have been steadily existing, although the proportion is low, and the emission reduction status of some regions is stable. As can be seen from 6(b), the overall regional carbon emission status is more in the growth state; combined with the change of α_{12}, it can be seen that some regions in the region gradually changed from the lowering to the growth state after 2013. The overall regional carbon emission status is stable during 2017~2019.

Figure 7 shows the probability change of the overall regional carbon emission development status in each consecutive 2 years. The state of growth is always more than the state of decrease, with growth between 2009 and 2010. 2010~2016 saw an improvement in the state of carbon emissions, with a partial change from growth to decrease.

2 Carbon emissions are linked to changes in economic and energy development status

Figure 8(a) shows that carbon emissions are in the lower state, b_{11} and b_{12} correspond to the lower state of economy and energy consumption, and the lower state of economic growth and energy consumption, which is very unlikely to occur from the macro historical data. The correlation between the growth state of carbon emissions and the growth state of economy and energy consumption is always high, and the b_{22} curve shows a 'rising trend' after 2017, which indicates that the correlation between the reduced state of carbon emissions and the reduced state of economy and the growth state of energy consumption is gradually increasing in a few regions, and it is necessary to identify these regions and take necessary measures to improve them.

Figure 6 Change in hidden state transfer probability, (a) hidden state transfer as a reduced probability change (b) hidden state transfer as a growth probability change (see online version for colours)

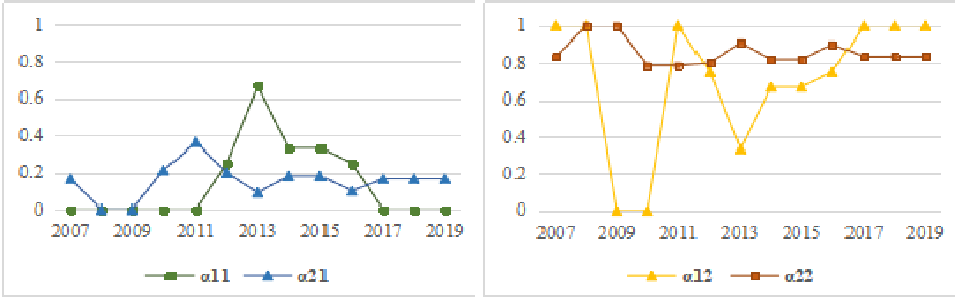

(a) (b)

Figure 7 Probability change of emission matrix based on time window (see online version for colours)

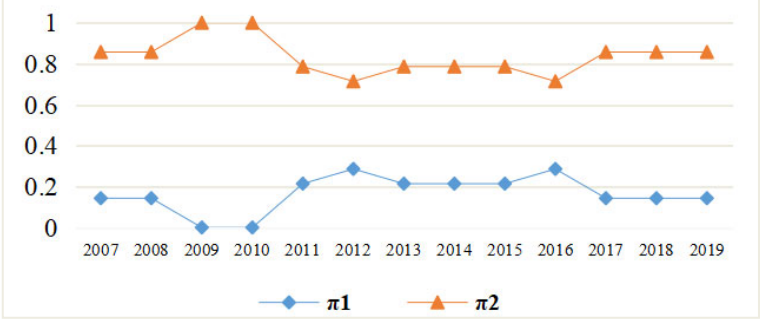

Figure 8 Observation state transfer probability change, (a) corresponding observation state probability change when the hidden state is reduced (b) corresponding observation state probability change when the hidden state is growth (see online version for colours)

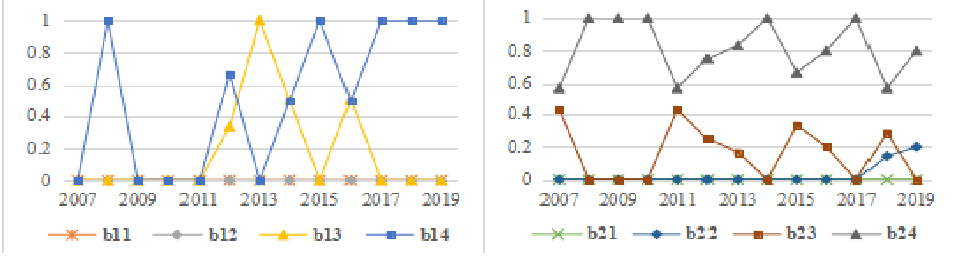

(a) (b)

4 Conclusions

In summary, the paper concludes as follows:

1 A method based on HMM for the dynamic influence relationship of multi-variables within a region is proposed. By setting a time window to optimise the HMM parameter estimation, the influence of state change among variables is highlighted; combined with the Viterbi algorithm to explore the best prediction effect of the hidden state that can be out, and realise the dynamic parameters to portray the multivariate state change law among regions, and the results are presented intuitively.

2 The overall prediction of carbon emission status in East China region was achieved based on the improved HMM, with an average correct rate of over 93%, and the best parameter estimation and prediction window consistent with the HMM of the region was obtained, which provides a research basis for the subsequent development of the prediction of future carbon emission status.

3 From the analysis of HMM dynamic parameters, it can be seen that the overall carbon emissions in East China region changed to a lower state more from 2009 to 2013, and part of the lower state gradually changed to a growth state after 2013; the lower state of carbon emissions began to correlate with the lower economic and energy consumption growth states from 2017 to 2019, and the correlation gradually increased.

Acknowledgements

The authors gratefully acknowledge the financial support from Open Research Fund of Anhui Province Key Laboratory of Green Building and Assembly Construction, Anhui Institute of Building Research and Design, Grant No. 2022-JKYL-003, the National Science Foundation of China No. 52268031, and the Doctoral initiation fund, Grant No. EA202211137.

References

Adedoyin, F.F. and Bekun, F.V. (2020) 'Modelling the interaction between tourism, energy consumption, pollutant emissions and urbanization: renewed evidence from panel VAR', *Environmental Science and Pollution Research*, Vol. 27, No. 31, pp.38881–38900.

Ağbulut, Ü. (2022) 'Forecasting of transportation-related energy demand and CO_2 emissions in Turkey with different machine learning algorithms', *Sustainable Production and Consumption*, Vol. 29, No. 14, pp.141–157.

Assis, A.L., Ricardo, F.J. and Mauro, R. (2023) 'Does monetary policy impact CO_2 emissions? A GVAR analysis', *Energy Economics*, Vol. 119, No. 11, pp.413–429.

CABBE (2021) *China Building Energy Consumption and Carbon Emissions Study [R/OL]*, 23 December [online] https://www.cabee.org/site/content/24237.html (accessed 26 October 2022).

Dong, B., Ma, X., Zhang, Z., Zhang, H., Chen, R., Song, Y., Shen, M. and Xiangm R. (2020) 'Carbon emissions, the industrial structure and economic growth: evidence from heterogeneous industries in China', *Environmental Pollution*, Vol. 262, No. 26, p.114322.

Dong, Z. and Chang, D. (2023) 'Accelerating and deepening environmental economic policy innovation and development, and building Chinese-style modernization with harmonious coexistence between man and nature', *Ecological Economics*, Vol. 39, No. 1, pp.25–30.

Du, Q., Deng, Y., Zhou, J., Wu, J. and Pang, Q. (2022) 'Spatial spillover effect of carbon emission efficiency in the construction industry of China', *Environmental Science and Pollution Research*, Vol. 29, No. 16, pp.2466–2479.

Du, Q., Shao, L., Zhou, J., Huang, N., Bao, T. and Hao, C. (2019) 'Dynamics and scenarios of carbon emissions in China's construction industry', *Sustainable Cities and Society*, Vol. 48, No. 27, p.101556.

Elmezain, M., Alwateer, M.M., El-Agamy, R., Atlam, E. and Ibrahim, H.M. (2023) 'Forward hand gesture spotting and prediction using HMM-DNN model', *Informatics*, Vol. 10, No. 1, p.1.

Grossman, G.M. and Krueger, A.B. (1995) 'Economic growth and the environment', *The Quarterly Journal of Economics*, Vol. 110, No. 2, pp.353–377.

Huang, S., Chung, Y. and Wu, T. (2021) 'Analyzing the relationship between energy security performance and decoupling of economic growth from CO_2 emissions for OECD countries', *Renewable and Sustainable Energy Reviews*, Vol. 152, No. 37, p.111633.

Jebli, M.B. and Youssef, S.B. (2017) 'Renewable energy consumption and agriculture: Evidence for cointegration and Granger causality for Tunisian economy', *International Journal of Sustainable Development & World Ecology*, Vol. 24, No. 2, pp.149–158.

Li, J. and Li, S. (2020) 'Energy investment, economic growth and carbon emissions in China – empirical analysis based on spatial Durbin model', *Energy Policy*, Vol. 140, No. 25, p.111425.

Li, W., Sun, W., Li, G., Cui, P., Wu, W. and Jin, B. (2017) 'Temporal and spatial heterogeneity of carbon intensity in China's construction industry', *Resources, Conservation and Recycling*, Vol. 126, No. 46, pp.162–173.

Li, W., Yang, G., Li, X., Sun, T. and Wang, J. (2019) 'Cluster analysis of the relationship between carbon dioxide emissions and economic growth', *Journal of Cleaner Production*, Vol. 225, No. 31, pp.459–471.

Lin, Q. and Yu, S. (2016) 'A spatial HMM approach for green networking', *Computer Communications*, Vol. 88, No. 15, pp.34–44.

Liu, Y., Zhang, J., Zhu, Z. and Zhao, G. (2019) 'Impacts of the 3E (economy, energy and environment) coordinated development on energy mix in China: the multi-objective optimisation perspective', *Structural Change and Economic Dynamics*, Vol. 50, No. 29, pp.56–64.

Manouchehri, N. and Bouguila, N. (2023) 'Human activity recognition with an HMM-based generative model', *Sensors*, Vol. 23, No. 3, p.1390.

Rey, S.J. (2001) 'Spatial empirics for economic growth and convergence', *Geographical Analysis*, Vol. 33, No. 3, pp.195–290.

Serdar, Ö., Volkan, H. and Bakim Ö. (2023) 'How do renewable energy, gross capital formation, and natural resource rent affect economic growth in G7 countries? Evidence from the novel GMM-PVAR approach', *Environmental Science and Pollution Research International*, Vol. 11, No. 46, pp.1721–1736.

Sosiawan, A.Y., Nooraeni, R. and Sari, L.K. (2021) 'Implementation of using HMM-GA in time series data', *Procedia Computer Science*, Vol. 179, pp.713–720.

Statistics Bureau of the People's Republic of China (2021) *China Statistical Yearbook*, China Statistics Press, Beijing.

Sun, J. and Zhang, H. (2021) 'Under the new development pattern evolution and the coordinated development of China regional gap research', *Journal of Economists*, Vol. 271, No. 7, pp.63–72.

Ulmeanu, A.P., Barbu, V.S., Tanasiev, V. and Badea, A. (2017) 'Hidden Markov models revealing the household thermal profiling from smart meter data', *Energy and Buildings*, Vol. 154, No. 18, pp.127–140.

Wang, K., Xu, R., Zhang, F., Miao, Z. and Pengm G. (2021) 'Spatiotemporal heterogeneity and driving factors of PM2.5 reduction efficiency: an empirical analysis of three urban agglomerations in the Yangtze River Economic Belt, China', *Ecological Indicators*, Vol. 132, No. 24, p.108308.

Wang, L., Yang, C., Sun, Y., Zhang, H. and Li, M. (2018) 'Effective variable selection and moving window HMM-based approach for iron-making process monitoring', *Journal of Process Control*, Vol. 68, No. 13, pp.86–95.

Wang, S., Huang, Y. and Zhou, Y. (2019) 'Spatial spillover effect and driving forces of carbon emission intensity at the city level in China', *Journal of Geographical Sciences*, Vol. 29, No. 13, pp.231–252.

Wen, L. and Yuan, X. (2020) 'Forecasting CO_2 emissions in China's commercial department, through BP neural network based on random forest and PSO', *Science of The Total Environment*, Vol. 718, No. 317, p.137194.

Xie, Z. (2021) 'Persisting in the strategic determination of actively responding to climate change and continuing to be an important participant, contributor and leader in the construction of global ecological civilization – commemorating the fifth anniversary of the Paris Agreement', *Environment and Sustainable Development*, Vol. 46, No. 1, pp.3–10.

Yan, S. and Chen, W. (2022) 'Analysis of the decoupling state and driving forces of China's construction industry under the carbon neutrality target', *Environmental Science and Pollution Research*, Vol. 29, No. 46, pp.78457–78471.

Yan, S. and Chen, W. (2022) 'Analysis of the decoupling state and driving forces of China's construction industry under the carbon neutrality target', *Environmental Science and Pollution Research*, Vol. 29, No. 49, pp.78457–78471.

Ye, L., Dang, Y., Fang, L. and Wang, J. (2023) 'Nonlinear interactive grey multivariable model based on dynamic compensation for forecasting the economy-energy-environment system', *Applied Energy*, Vol. 331, No. 21, p.120189.